Effect of Deep-Acceptor Density in Buffer Layer on Breakdown Voltage of AlGaN/GaN HEMTs with High-*k* Passivation Layer

S. Ueda, Y. Kawada, and K. Horio

Faculty of Systems Engineering, Shibaura Institute of Technology
307 Fukasaku, Minuma-ku, Saitama 337-8570, Japan, horio@sic.shibaura-it.ac.jp

ABSTRACT

We make a numerical analysis of breakdown characteristics of AlGaN/GaN HEMTs with a high-*k* passivation layer, where a deep acceptor above the midgap is considered in a buffer layer and its density N_{DA} is varied between 10^{17} and $3x10^{17}$ cm^{-3}. It is shown that, generally, the breakdown voltage V_{br} becomes higher when the relative permittivity of the passivation layer ε_r is higher. In the case where N_{DA} is relatively low, V_{br} is determined by impact ionization of carriers when ε_r is low, but it becomes determined by buffer leakage current when ε_r is high, and V_{br} becomes saturated with increasing ε_r. On the other hand, when N_{DA} is relatively high, V_{br} is determined by impact ionization of carriers even if ε_r becomes 60, and it becomes about 500 V at the gate-to-drain distance of 1.5 μm, which corresponds to an average electric field of over 3 MV/cm.

Keywords: GaN HEMT, breakdown voltage, buffer latyer, deep acceptor, high-*k* passivation layer

1 INTRODUCTION

AlGaN/GaN HEMTs are now receiving great interest for application to high-power microwave devices and high power switching devices [1, 2]. To improve the power performance and the breakdown voltage of FETs, the introduction of field plate is shown to be effective [3-8], but it may increase the parasitic capacitance, leading to degrading the high-frequency performance. In a previous work [9, 10], as another method to improve the breakdown voltage of AlGaN/GaN HEMTs, we proposed a structure including a high-*k* passivation layer, and showed that the breakdown voltage increased significantly. We assumed an undoped semi-insulating buffer layer where a deep donor compensates a deep acceptor. Recently, Fe- and C-doped semi-insulating buffer layers are often adopted and they acts as deep acceptors [11-15]. Therefore, in this work, we analyze AlGaN/GaN HEMTs with a buffer layer including only a deep acceptor, and studied how the breakdown voltage is influenced by its density.

2 PHYSICAL MODEL

A device structure analyzed here is shown in Fig.1. The gate length and the gate-to- drain distance is 0.3 μm and 1.5 μm, respectively. The passivation layer's thickness is 0.1 μm. We vary the relative permittivity of the passivation layer ε_r as a parameter. Here, we adopt a Fe-doped semi-insulating buffer layer, where the Fe-related level (E_{DA}) is set to 0.5 eV below the bottom of conduction band [11, 15]. The Fe-related level is a deep acceptor. The deep acceptors act as electron traps. The deep-acceptor density N_{DA} is varied between 10^{17} and $3x10^{17}$ cm^{-3}.

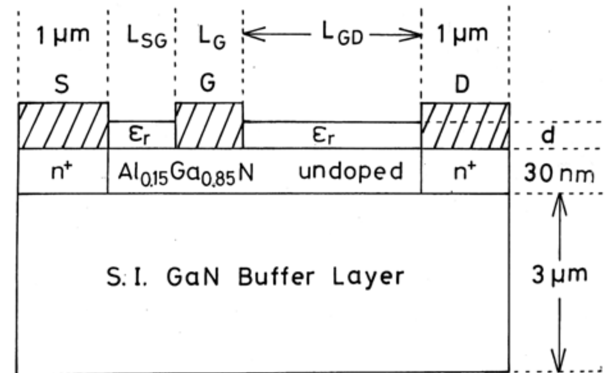

Figure 1: Device structure analyzed in this study.

Basic equations to be solved are Poisson's equation having the ionized deep-acceptor density term and electron and hole continuity equations which include a carrier loss rate via the deep acceptor and an impact ionization rate [10, 16-18] and expressed as follows.

1) Poisson's equation

$$\nabla \bullet (\varepsilon \nabla \psi) = -q(p - n + N_{Di} - N_{DA}^{-}) \quad (1)$$

2) Continuity equations for electrons and holes

$$\nabla \bullet J_n = -qG + qR_{DA} \quad (2)$$

$$\nabla \bullet J_p = qG - qR_{DA} \quad (3)$$

where N_{DA}^{-} is the ionized deep-acceptor density, and R_{DA} represents a carrier recombination rate via the deep acceptor. G is a carrier generation rate by impact ionization, and given by

$$G = (\alpha_n \mid J_n \mid + \alpha_p \mid J_p \mid) / q \quad (4)$$

where α_n and α_p are ionization rates for electrons and holes, respectively, and expressed as

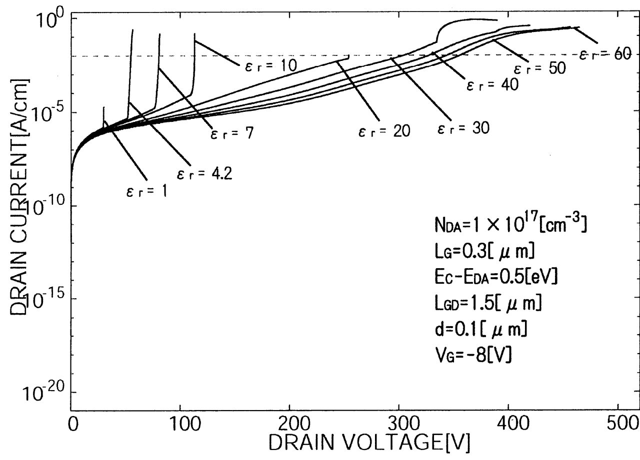

(a)

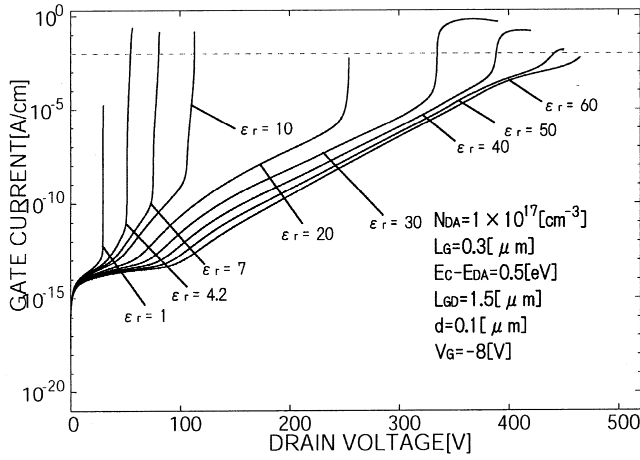

(b)

Figure 2: Calculated off-state (a) $I_D - V_D$ curves and (b) $I_G - V_D$ curves when $N_{DA} = 10^{17}$ cm^{-3}. The dotted lines indicate 1 mA/mm.

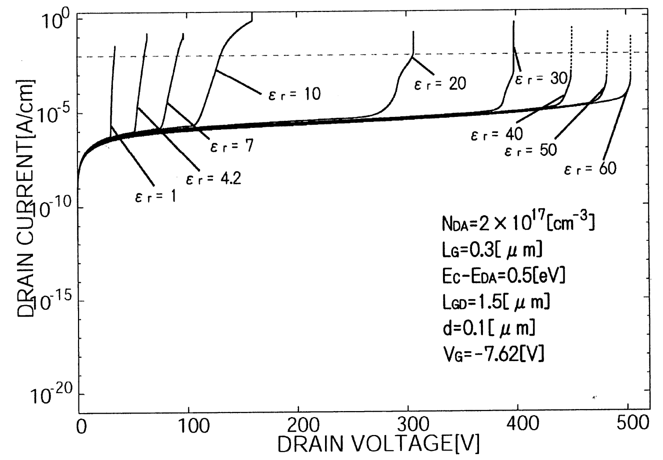

(a)

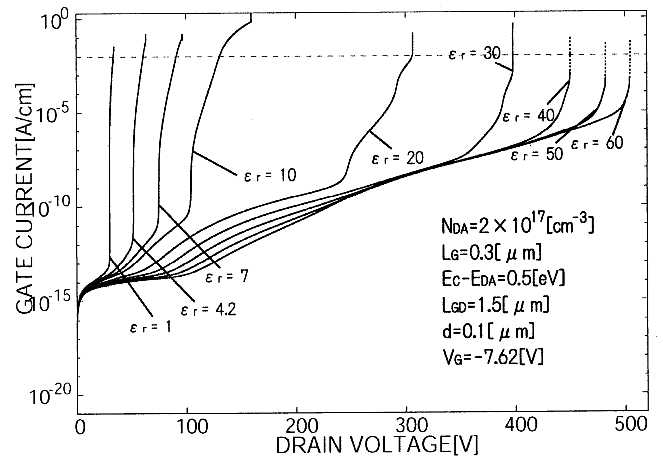

(b)

Figure 3: Calculated off-state (a) $I_D - V_D$ curves and (b) $I_G - V_D$ curves when $N_{DA} = 2\text{x}10^{17}$ cm^{-3}. The dotted lines indicate 1 mA/mm.

$$\alpha_n = A_n \exp(-B_n / | E |) \tag{5}$$

$$\alpha_p = A_p \exp(-B_p / | E |) \tag{6}$$

where E is the electric field. A_n, B_n, A_p, and B_p are deduced from [19].

The above basic equations are put into discrete forms and solved numerically.

3 RESULTS AND DISCUSSIONS

Figs.2 and 3 and shows calculated drain current (I_D) – drain voltage (V_D) curves and gate current (I_G) -V_D curves as a parameter of the relative permittivity of passivation layer ε_r, where N_{DA} is 10^{17} and $2\text{x}10^{17}$ cm^{-3}, respectively. In both cases, when ε_r is low (≤ 10), a sudden increase in drain current due to impact ionization determines the breakdown voltage V_{br}. Here the drain current becomes equal to the gate current. In the case of $N_{DA} = 10^{17}$ cm^{-3}, when ε_r becomes high (≥ 30), I_D reach a critical value (1 mA/mm) before a sudden increase in I_D. In this case the drain current is much higher than the gate current, and hence the buffer leakage current determines V_{br}. Note that V_{br} is defined here as the drain voltage when I_D becomes 1 mA/mm. In Figs.2 and 3, V_{br} increases as ε_r increases. This is because the electric field at the drain edge of the gate is reduced when ε_r becomes high [13]. In the case of $N_{DA} = 2\text{x}10^{17}$ cm^{-3}, even if ε_r becomes high (≥ 30), I_D increase suddenly due to impact ionization of carriers and I_D is nearly equal to I_G in this region.

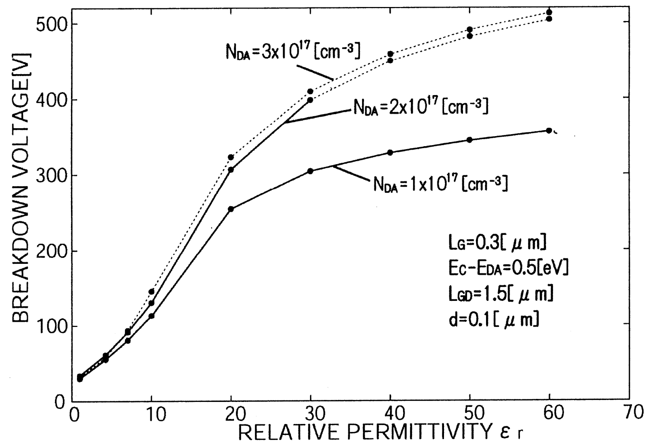

Figure 4: Comparison of breakdown voltage V_{br} versus ε_r curves among the three cases with different N_{DA}.

Fig.4 compares the breakdown voltage V_{br} versus ε_r curves among the three cases with different N_{DA}. In the case of N_{DA} = 2x10^{17} cm^{-3} and 3x10^{17} cm^{-3}, V_{br} becomes much higher than that for N_{DA} = 10^{17} cm^{-3} when ε_r becomes higher than 30. This is because the buffer leakage current is reduced for N_{DA} = 2x10^{17} cm^{-3} and 3x10^{17} cm^{-3} and V_{br} becomes determined by impact ionization of carriers. In the case of ε_r is 60, V_{br} reaches about 500 V, which corresponding to the average electric field of 3.3 MV/cm between the gate and the drain.

Fig.5 shows electric field profiles at the heterojunction interface between the two cases with N_{DA} = 10^{17} and 2x10^{17} cm^{-3}. Here, ε_r is 40. The electric field profiles are similar between the two cases until V_D = 327 V which is the breakdown voltage for N_{DA} = 10^{17}, and it is determined by the buffer leakage current. In the case of N_{DA} = 2x10^{17} cm^{-3}, the breakdown voltage is 450 V which is determined by impact ionization of carriers at the drain edge of the gate region. The electric field profiles are rather uniform in this case. It is concluded that the difference of buffer leakage current is essential to determine the difference of breakdown voltage here.

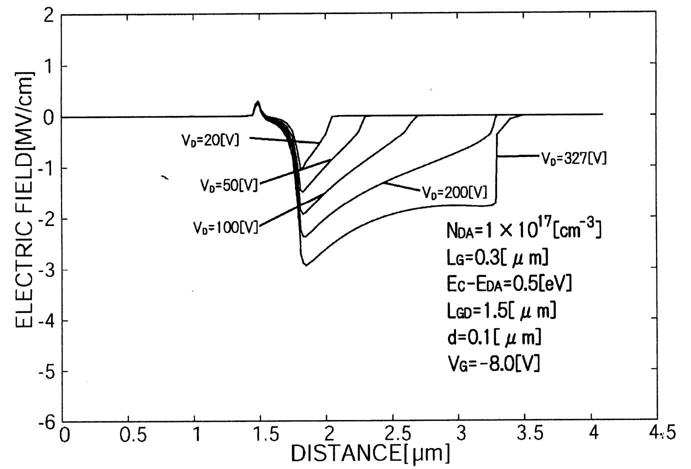

(a)

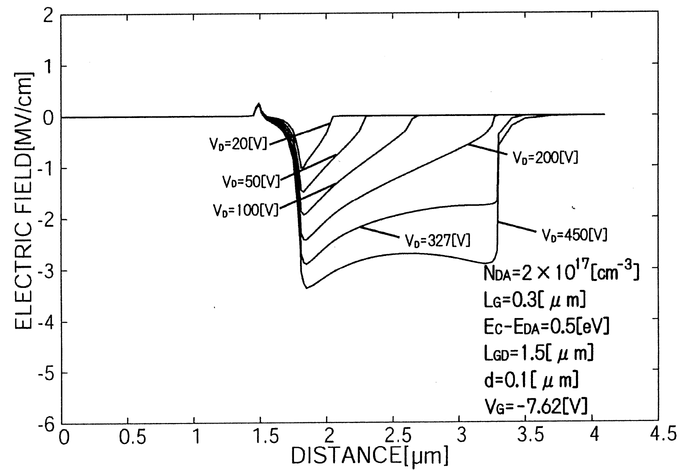

(b)

Figure 5: Comparison of electric field profiles along the heterojunction interface. ε_r = 40. (a) N_{DA} = 10^{17} cm^{-3}, (b) N_{DA} = 2x10^{17} cm^{-3}.

4 CONCLUSION

A two-dimensional numerical analysis of off-state breakdown characteristics in AlGaN/GaN HEMTs with a high-*k* passivation layer has been performed, where a deep acceptor above the midgap is considered in the buffer layer. Its density N_{DA} is varied between 10^{17} and 3x10^{17} cm^{-3}. It has been ascertained that the breakdown voltage V_{br} becomes higher when the relative permittivity of the passivation layer ε_r is higher. When N_{DA} is 10^{17} cm^{-3}, V_{br} is determined by impact ionization of carriers when ε_r is low, but it becomes determined by buffer leakage current when ε_r is high. In this case, V_{br} becomes almost saturated with ε_r. On the other hand, when N_{DA}= 2 ~ 3x10^{17} cm^{-3}, the buffer leakage current is reduced and hence V_{br} is determined by impact ionization of carriers even if ε_r becomes 60. In this case V_{br} reaches about 500 V at the gate-to-drain distance of 1.5 μm, which corresponds to an average electric field of over 3 MV/cm.

REFERENCES

[1] U. K. Mishra, L. Shen, T. E. Kazior, and Y.-F. Wu, “GaN-based RF power devices and amplifiers”, Proc. IEEE, vol.96, pp.287-305, 2008.

[2] N. Ikeda, Y. Niiyama, H. Kambayashi, Y. Sato, T. Nomura, S. Kato, and S. Yoshida, “GaN power transistors on Si substrates for switching applications”, Proc. IEEE, vol.98, pp.1151-1161, 2010.

[3] A. Wakejima, K. Ota, K. Matsunaga, and M. Kuzuhara, "A GaAs-based field-modulating plate HFET with improved WCDMA peak-output-power characteristics", IEEE Trans. Electron Devices, vol.50, pp.1983-1987, Sep. 2003

[4] Y.-F. Wu, A. Saxler, M. Moore, R. P. Smith, S. Sheppard, P. M. Chavarkar, T. Wisleder, U. K. Mishra, and P. Parikh, "30-W/mm GaN HEMTs by field plate optimization", IEEE Electron Device Lett., vol.25, pp.117-119, 2004.

[5] K. Horio, A. Nakajima, and K. Itagaki, "Analysis of field-plate effects on buffer-related lag phenomena and current collapse in GaN MESFETs and AlGaN/GaN HEMTs", Semicond. Sci. Technol., vol.24, pp.085022-1–085022-7, 2009.

[6] K. Horio, T. Tanaka, K. Itagaki and A. Nakajima, "Two-dimensional analysis of field-plate effects on surface state-related current transients and power slump in GaAs FETs", IEEE Trans. Electron Devices, vol.58, pp. 698-703, 2011.

[7] S. Karmalkar and U. K. Mishra, "Enhancement of breakdown voltage in AlGaN/GaN high electron mobility transistors using a field plate", IEEE Trans. Electron Devices, vol.48, pp.1515-1521, 2001.

[8] H. Onodera and K. Horio, "Analysis of buffer-impurity and field-plate effects on breakdown characteristics in small sized AlGaN/GaN high electron mobility transistors", Semicond. Sci. Technol., vol.27, pp.085016-1–085016-6, 2012.

[9] H. Hanawa and K. Horio, "Increase in breakdown voltage of AlGaN/GaN HEMTs with a high-*k* dielectric layer", Phys. Status Solidi A, vol.211, pp.784-787, 2014.

[10] H. Hanawa, H. Onodera, A. Nakajima, and K. Horio, "Numerical analysis of breakdown voltage enhancement in AlGaN/GaN HEMTs with a high-*k* passivation layer", IEEE Trans. Electron Devices, vol.61, pp.769-775, 2014.

[11] M. Silvestri, M. J. Uren, and M. Kuball, "Iron-induced deep-acceptor center in GaN/AlGaN high electron mobility transistors: Energy level and cross section", Appl. Phys. Lett. Vol.102, pp.073051-1–073051-4, 2013.

[12] G. Verzellesi, L. Morassi, G. Meneghesso, M. Meneghini, E. Zanoni, G. Pozzovivo, S. Lavanga, T. Detzel, O. Häberlen, and G. Curatola, "Influence of carbon doping on pulsed and AC behavior of insulated-gate field-plated power AlGaN/GaN HEMTs", IEEE Electron Device Lett. vol.35, pp.443-445, 2014.

[13] S. Gusafsson, Jr-T. Chen, J. Bergten, U. Forsberg, M. Thorsell, E. Janzén, and N. Rorsman, "Dispersive effects in microwave AlGaN/AlN/GaN HEMTs with carbon-doped buffer", IEEE Trans. Electron Devices, vol.62, pp.2162-2169, 2015.

[14] J. Hu, S. Stoffels, S. Lenci, G. Groeseneken, and S. Decoutere, "On the identification of buffer trapping for bias-dependent dynamic R_{ON} of AlGaN/GaN Schottky barrio diode with AlGaN:C back barrier", IEEE Electron Device Lett., vol.37, pp.310-313, 2016.

[15] Y. S. Puzyrev, R. D. Schrimpf, D. M. Fleetwood, and S. T. Pantelides, "Role of Fe impurity complexes in the degradation of GaN/AlGaN high-electron mobility transistors", Appl. Phys. Lett., vol.106, pp.053505-1–053505-4, 2015.

[16] K. Horio and K. Satoh, "Two-dimensional analysis of substrate-related kink phenomena in GaAs MESFET's", IEEE Trans. Electron Devices, vol.41, pp.2256-2261, 1994.

[17] K. Horio and A. Wakabayashi, "Numerical analysis of surface-state effects on kink phenomena of GaAs MESFETs", IEEE Trans. Electron Devices, vol.47, pp.2270-2276, 2000.

[18] Y. Mitani, D. Kasai and K. Horio, "Analysis of surface-state and impact-ionization effects on breakdown characteristics and gate-lag phenomena in narrowly-recessed-gate GaAs FETs", IEEE Trans. Electron Devices, vol.50, pp.285-291, 2003.

[19] C. Bulutay, "Electron initiated impact ionization in AlGaN alloys", Semicond. Sci. Technol., vol.17, pp.59-62, 2002.